

Impact of Polar Ozone Depletion on Subtropical Precipitation

S. M. Kang,^{1*} L. M. Polvani,^{1,2} J. C. Fyfe,³ M. Sigmond⁴

¹Department of Applied Physics and Applied Mathematics, Columbia University, New York, NY, USA. ²Department of Earth and Environmental Sciences, Columbia University, New York, NY, USA. ³Canadian Centre for Climate Modelling and Analysis, Environment Canada, Victoria, British Columbia, Canada. ⁴Department of Physics, University of Toronto, Toronto, Ontario, Canada.

*To whom correspondence should be addressed. E-mail: smk2182@columbia.edu

Over the past half-century, the ozone hole has caused a poleward shift of the extratropical westerly jet in the Southern Hemisphere. Here, we argue that these extratropical circulation changes, resulting from ozone depletion, have substantially contributed to subtropical precipitation changes. Specifically, we show that precipitation in the Southern subtropics in austral summer increases significantly when climate models are integrated with reduced polar ozone concentrations. Furthermore, the observed patterns of subtropical precipitation change, from 1979 to 2000, are very similar to those in our model integrations, where ozone depletion alone is prescribed. In both climate models and observations, the subtropical moistening is linked to a poleward shift of the extratropical westerly jet. Our results highlight the importance of polar regions on the subtropical hydrological cycle.

The Southern Hemisphere mid-to-high latitude circulation has undergone marked climate change over the past few decades (1–2). One of the most pronounced features is a poleward displacement of the Southern Hemisphere westerly jet, which has been accompanied by a poleward shift of mid-to-high latitude precipitation associated with the extratropical storm track (3–6). Modeling and observational studies have demonstrated that in austral summer these Southern Hemisphere trends have been caused largely by stratospheric ozone depletion, with a smaller contribution from an increased atmospheric concentration of well-mixed greenhouse gases (7–13).

Although these mid-to-high latitude circulation changes have been the focus of most recent studies on the impact of the ozone hole, several hints of its impacts on the tropics can be found in the literature. For instance, a poleward shift of the southern edge of the Hadley cell has been reported (8, 9, 13), as well as a change in the latitude of the poleward edge of the subtropical dry zones (8). Furthermore, in both observations and climate models, poleward displacements in the latitude of the Southern Hemisphere westerly jet have been linked to the expansion of subtropical dry zones (14), as well as to

increased rainfall over eastern Australia and southern South Africa (15). Since the Southern Hemisphere westerly jet in austral summer is influenced by ozone depletion, one may suspect that the ozone hole might play an important role not only in the extratropical circulation but also in the hydrological cycle at lower latitudes. Indeed, during the period of ozone depletion between 1979 and 2000, observations (Fig. 1A) exhibit a very noticeable moistening trend in austral summer in the subtropical band between 15–35°S (highlighted box); this is even clearer in the zonal mean (Fig. 1B). The aim of this paper is to use state-of-the-art climate models to demonstrate that stratospheric ozone depletion over the South Pole has contributed to the observed change in subtropical precipitation.

It is well known that results pertaining to precipitation can be highly model dependent. In view of this, we use two independently developed climate models that are very different in their physical parameterizations (16). One is the Canadian Middle Atmosphere Model (CMAM) (17), and the other the NCAR Community Atmospheric Model (CAM3) (18). All experiments presented here consist of pairs of so-called “time-slice” integrations with prescribed monthly-varying ozone concentrations (16): one “reference” integration which uses ozone fields prior to the formation of the ozone hole, and one “ozone hole” integration in which stratospheric ozone is severely depleted, notably over the South Pole. The climate response to ozone depletion is obtained by differencing the climatologies of these two integrations.

Experiments were conducted with four distinct model configurations: (i) the coupled CMAM with interactive ocean and sea ice, (ii) the uncoupled CMAM with prescribed monthly-mean annually-varying sea surface temperatures and sea ice concentrations taken from the coupled reference integration, (iii) the uncoupled CAM3 with observed sea surface temperatures and sea ice concentrations averaged over the pre-ozone hole period (19), and (iv) the uncoupled CAM3 but with ozone changes confined to latitudes southward of 40°S. These substantially different

configurations allow us to evaluate whether the effect of ozone depletion on subtropical precipitation is fundamentally dependent on atmosphere-ocean interactions and physical model parameterizations. Experiment (iv) is crucial in determining whether polar or subtropical ozone depletion is the key player.

The impact of the ozone hole on precipitation is clearly evident in Fig. 2, where the response due to the ozone depletion is shown for each of the four experiments, in austral summer. First, note the considerable similarity among the four experiments: this confirms the robustness of our result. As reported in previous studies (8, 9, 20), there is decreased precipitation around 45°S, and increased precipitation around 60°S, associated with a poleward-shifted storm track. The focus of this paper, however, is the ozone-hole induced moistening (green patches) in the highlighted region of the subtropics, most pronounced over the southwestern Indian Ocean, eastern Australia, and southern flank of the Southern Pacific Convergence Zone (SPCZ) where the climatological mean precipitation is large. In these regions, our models show that the precipitation response to the ozone hole is unaffected by atmosphere-ocean interactions (contrast Fig. 2, A and B), is largely independent of the physical parameterizations of any one model or the sea surface temperatures used (contrast Fig. 2, B and C), and originates almost entirely from ozone depletion in the Southern polar regions (contrast Fig. 2, C and D).

Second, contrast the modelled ozone-hole induced precipitation changes in Fig. 2 with the observed changes in Fig. 1A. While the observed changes in precipitation at individual tropical locations are generally larger in magnitude than in our experiments, there is good agreement in the overall patterns. Spatial agreement is strikingly evident in the zonal mean profiles (contrast Fig. 1B with Fig. 3A), all of which show a very clear tripole pattern consisting of high-latitude moistening, mid-latitude drying, and subtropical moistening. Between 15-35°S these precipitation changes correspond to about a 10% increase relative to the climatology, with larger increases in some subregions. We emphasize that the increased precipitation in the highlighted 15-35°S region is statistically significant in observations and in all four experiments. As an example, in Fig. 3A we show the 95% confidence interval (red shading) for one of the CAM3 experiments; this interval is computed using the Student's *t*-test, assuming independent and randomly distributed residuals. Furthermore, as shown in Fig. 3B, these subtropical precipitation changes are largely associated with changes in moisture convergence by the time-mean zonal-mean flow (with smaller contributions from transient and stationary eddies), rather than to local changes in atmospheric humidity (fig. S1). In Fig. 3C we further show, from a regression of precipitation on jet latitude, that these

subtropical precipitation changes are highly congruent with changes in the latitude of the extratropical westerly jet (16). Moreover note that, as in our model experiments, the observed moistening in the 15-35°S region is also linked to a poleward jet shift (Fig. 1B), which itself is substantially the consequence of polar ozone depletion (1, 3, 8).

We next elucidate the mechanism causing these subtropical precipitation changes. The zonal-mean changes due to ozone depletion in temperature, zonal wind, and mean meridional mass streamfunction are shown in Fig. 4. For brevity we show only results for the coupled CMAM (top row), and the uncoupled CAM3 with high-latitude ozone depletion only (bottom row); the other two experiments are very similar. Ozone depletion causes severe cooling in the lower stratosphere (Fig. 4, A and D), which in turn is accompanied by a lifting of the polar tropopause and a concomitant poleward shift of the extratropical westerly jet (Fig. 4, B and E). This sequence of high-to-mid latitude cause and effect is well documented (11).

The poleward shift of the extratropical westerly jet is reflected in the convergence and divergence of transient eddy momentum fluxes on its poleward and equatorward flanks, respectively (fig. S3). This poleward jet shift is also associated with a poleward shift of the subtropical edge of the Hadley cell (seen as the blue/red shading centered around 25°S in Fig. 4, C and F). Accompanying the poleward shift of this edge, an anomalous upper-level mass divergence between 15-35°S is found, and it is largely associated with changes in the transient eddy momentum fluxes (fig. S4). This upper-level divergence drives anomalous rising motion in the subtropics (arrows around 25°S in Fig. 4, C and F), inducing low level moisture convergence and hence increased precipitation there. In short, our experiments expose a sequence of high-to-low latitude causes and effects linking stratospheric polar ozone depletion all the way to subtropical moistening. This mechanism does not, however, explain the longitudinal variations in the precipitation response seen in Fig. 2: these will need to be addressed in a future study.

We recognize that other radiative agents, such as anthropogenic greenhouse gases or sulphate aerosols, may have also played a role in changing precipitation at low latitudes. This has been confirmed in a recent study (21), where observed twentieth century changes in annual-mean and zonal-mean land precipitation were linked to anthropogenic greenhouse gas and sulphate aerosol forcings. That study noted, in addition, that models tend to underestimate the magnitude of the observed changes, especially at low latitudes. Similar discrepancies in amplitude were reported with precipitation responses to volcanic eruption (22). In our study, we find that both the pattern and the magnitude of zonal mean precipitation changes in austral summer agree well between observations and climate models

forced with polar ozone depletion alone. This, therefore, strongly implicates polar stratospheric ozone depletion as being an important driver of the Southern subtropical moistening observed in austral summer over the latter part of the twentieth century.

In a broader perspective, the impact of polar ozone depletion on tropical precipitation discussed here provides one more instance of how changes in high latitudes are able to affect the tropics. Other well-known examples are the effect of Arctic sea ice (23) and of the Atlantic thermohaline circulation (24) on the position of the Intertropical Convergence Zone (ITCZ). Hence the need to deepen our understanding of polar to tropical linkages in order to accurately predict tropical precipitation.

References and Notes

1. D. W. J. Thompson, S. Solomon, *Science* **296**, 895 (2002).
2. K. Trenberth, P. Jones, and coauthors, *Climate change 2007: The physical science basis. Contribution of working group I to the Fourth Assessment Report of the Intergovernmental Panel on Climate Change* (2007).
3. R. L. Fogt et al., *Journal of Climate* **22**, 5346 (2009).
4. G. J. Marshall, *Journal of Climate* **16**, 4134 (2003).
5. D. W. J. Thompson, J. M. Wallace, G. C. Hegerl, *Journal of Climate* **13**, 1018 (2000).
6. C. Archer, K. Caldeira, *Geophys. Res. Lett.* **35**, L08803 (2008).
7. J. M. Arblaster, G. A. Meehl, *Journal of Climate* **19**, 2896 (2006).
8. L. M. Polvani, D. W. Waugh, G. J. P. Correa, and S.-W. Son, *Journal of Climate* **24**, 795 (2011).
9. S.-W. Son, N. F. Tandon, L. M. Polvani, D. W. Waugh, *Geophys. Res. Lett.* **36**, L15705 (2009).
10. N. P. Gillett, D. W. J. Thompson, *Science* **302**, 273 (2003).
11. S. W. Son et al., *Science* **320**, 1486 (2008).
12. J. Perlwitz, S. Pawson, R. L. Fogt, J. E. Nielsen, W. D. Neff, *Geophys. Res. Lett.* **35**, L08714 (2008).
13. S. W. Son et al., *J. Geophys. Res.* **115**, D00M07 (2010).
14. M. Previdi, B. G. Liepert, *Geophys. Res. Lett.* **34**, L22701 (2007).
15. A. Sen Gupta, M. H. England, *Journal of Climate* **19**, 4457 (2006).
16. Materials and methods are available as supporting material on Science Online.
17. J. F. Scinocca, N. A. McFarlane, M. Lazare, J. Li, and D. Plummer, *Atmos. Chem. Phys.* **8**, 7055 (2008).
18. W. D. Collins et al., *Journal of Climate* **19**, 2122 (2006).
19. N. A. Rayner et al., *J. Geophys. Res.* **108**, 4407 (2003).
20. M. Sigmond, J. C. Fyfe, J. F. Scinocca, *Geophys. Res. Lett.* **37**, L12706 (2010).
21. X. Zhang et al., *Nature* **448**, 461 (2007).
22. N. P. Gillett, A. J. Weaver, F. W. Zwiers, M. F. Wehner, *Geophys. Res. Lett.* **31**, L12217 (2004).
23. J. C. H. Chiang, and C. M. Bitz, *Climate Dynamics* **25**, 477 (2005).
24. R. Zhang, T. L. Delworth, *Journal of Climate* **18**, 1853 (2005).
25. R. F. Adler et al., *Journal of Hydrometeorology* **4**, 1147 (2003).
26. S. M. Uppala et al., *Quarterly Journal of the Royal Meteorological Society* **131**, 2961 (2005).
27. R. Kistler et al., *Bulletin of the American Meteorological Society* **82**, 247 (2001).

Acknowledgements: We are grateful to I. Held, D. Frierson, A. Sobel, G. Flato, B. Merryfield and N. Gillett for comments on early versions of this work. L.M.P. and S.M.K. are supported in part by a grant from the US National Science Foundation to Columbia University. M.S. is a member of the CSPARC network, and gratefully acknowledges the support of the Canadian Foundation for Climate Atmospheric Sciences.

Supporting Online Material

www.sciencemag.org/cgi/content/full/science.1202131/DC1
Materials and Methods

SOM Text

Figs. S1 to S4

References

23 December 2010; accepted 8 April 2011

Published online 21 April 2011; 10.1126/science.1202131

Fig. 1. Observed precipitation change between 1979 and 2000 in austral summer (December to February mean). **(A)** Precipitation change based on GPCP data (25), calculated from the linear trend multiplied by 22 years. Black contours show the mean precipitation for 1979-1983, with contour interval of 3 mm day⁻¹. **(B)** Zonal-mean precipitation change (red line) with 95% confidence interval (red shading), and the change congruent (16) with a change in the latitude of the westerly jet obtained from ERA40 (26) (blue line) and NCEP/NCAR (27) (green line) reanalysis data.

Fig. 2. Modelled precipitation change caused by the ozone hole. Shading shows austral summer precipitation difference (in mm day⁻¹) induced by ozone depletion in **(A)** the coupled CMAM, **(B)** the uncoupled CMAM, **(C)** the uncoupled CAM3, and **(D)** the uncoupled CAM3 with ozone depletion confined to 40-90°S. Black contours show the mean precipitation in the respective reference integrations, with contour interval of 3 mm day⁻¹. Locations where the response is significant at the 95% confidence level are hatched.

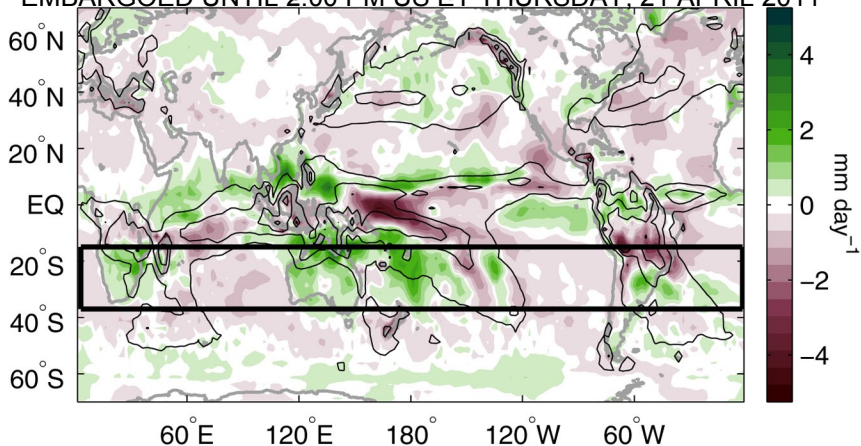
Fig. 3. Modelled zonal-mean change caused by the ozone hole. **(A)** Precipitation change, **(B)** mean moisture

convergence change and (C) precipitation change congruent with the change in extratropical westerly jet latitude (16). All panels are for austral summer, with the 95% confidence interval shown in red shading for experiment (iii).

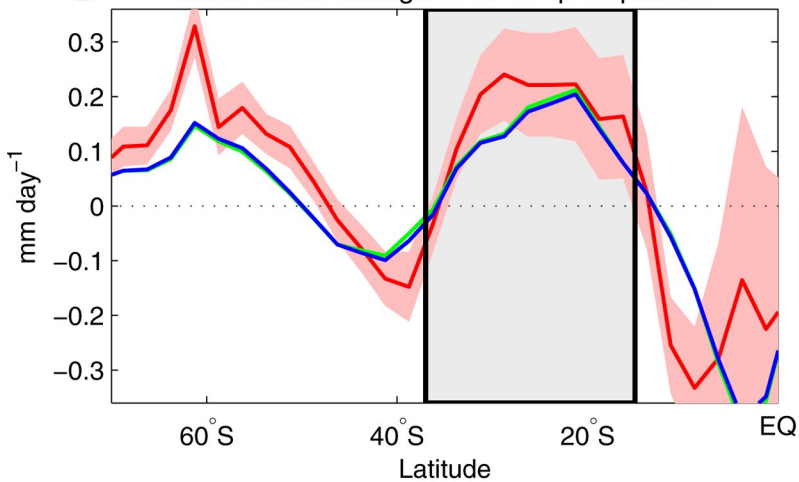
Fig. 4. Mechanism linking the ozone hole to subtropical precipitation change. Shading is the zonal-mean response in austral summer of (A and D), temperature (in K), (B and E), zonal wind (in m s^{-1}), and (C and F), mean meridional mass streamfunction (in 10^9 kg s^{-1}). Black solid contours in (A) and (D) are the mean temperatures, and red dashed lines indicate the tropopause height in the reference integrations; the arrows illustrate the lifting of tropopause in response to ozone depletion. Black solid (dashed) contours in (B) and (E) are the mean westerlies (easterlies) in the reference integrations, and the arrows illustrate the direction of extratropical westerly jet shift. Black solid (dashed) contours in (C) and (F) are the clockwise (counter-clockwise) mean meridional circulation in the reference integrations, and the arrows illustrate the direction of anomalous vertical motion induced by ozone depletion. Top row: the coupled CMAM integrations [experiment (i)]. Bottom row: the uncoupled CAM3 integrations with ozone depletion confined to 40-90°S [experiment (iv)].

A Change in GPCP precipitation

EMBARGOED UNTIL 2:00 PM US ET THURSDAY, 21 APRIL 2011



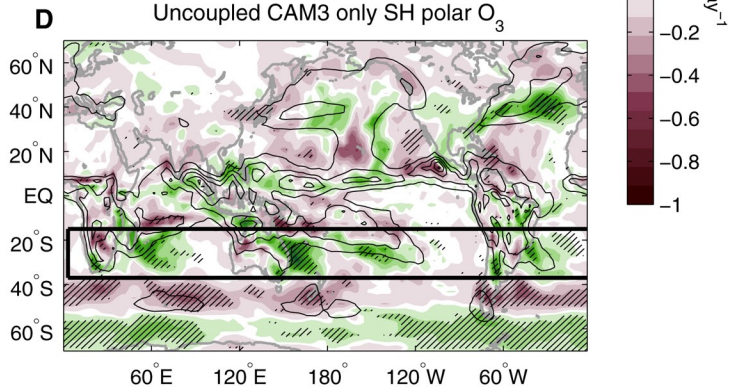
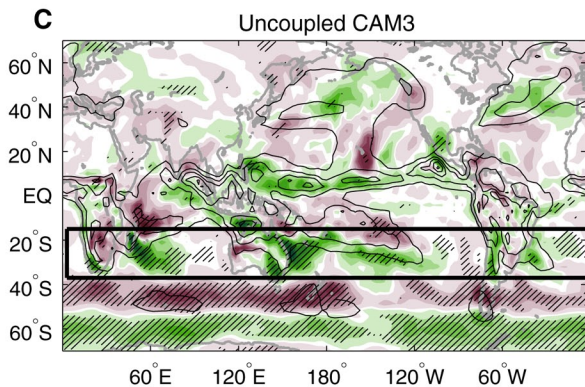
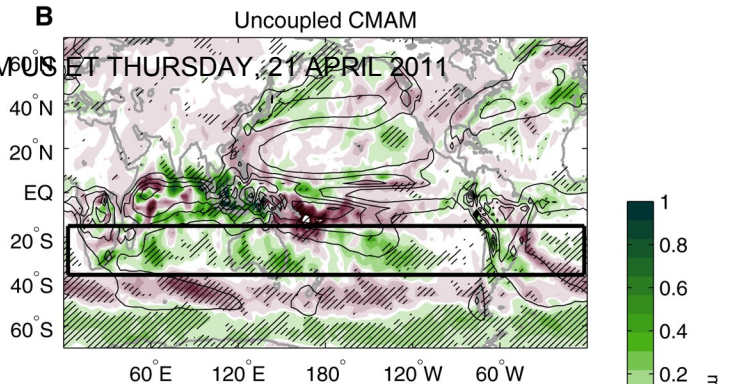
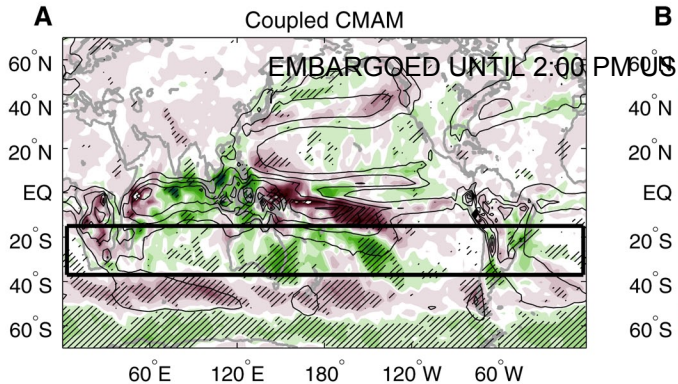
B Zonal mean change in GPCP precipitation

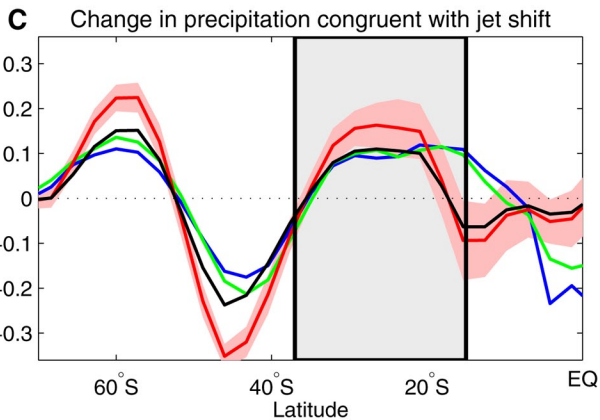
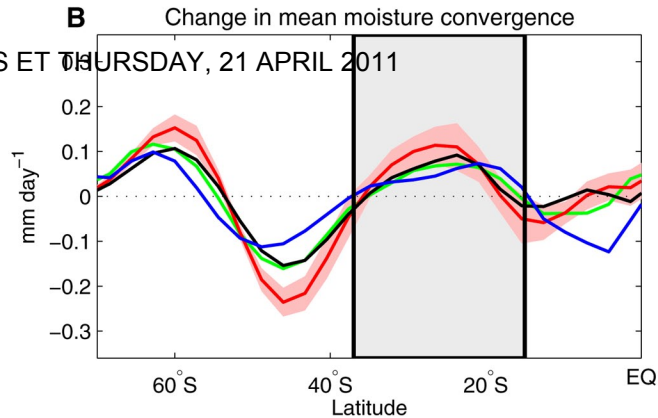
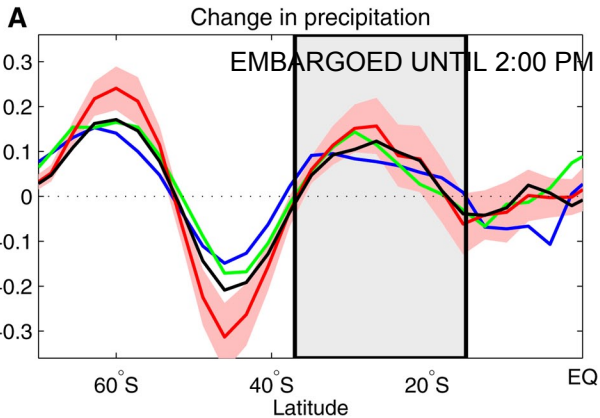


— Total

— Congruent with jet shift (ERA40 u)

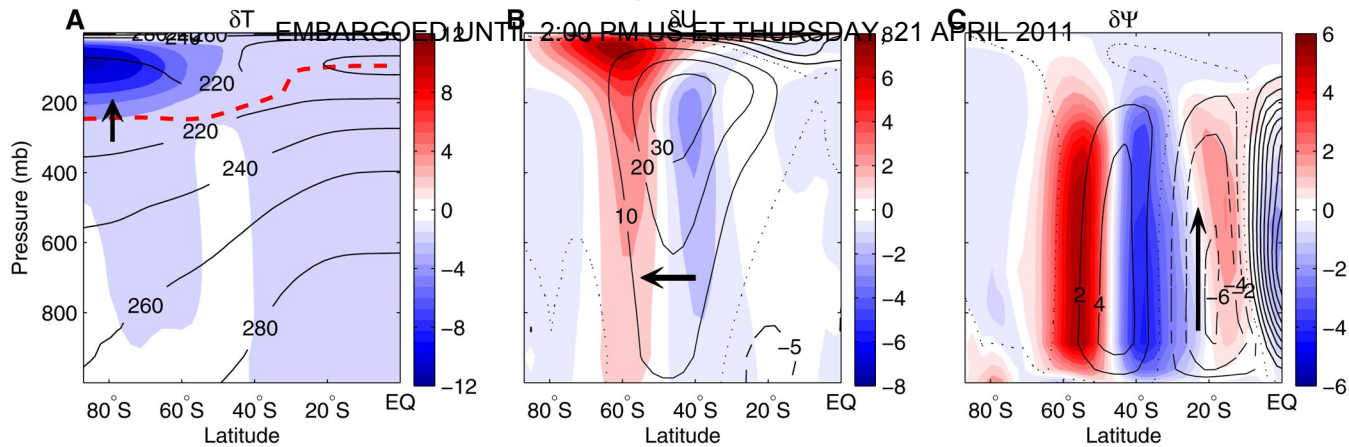
— Congruent with jet shift (NCEP u)





- Coupled CMAM
- Uncoupled CMAM
- Uncoupled CAM3
- Uncoupled CAM3 only SH polar O₃

Coupled CMAM



Uncoupled CAM3 only SH polar O₃

